Stabilization of the bunch position during the control of the microbunching instability in storage rings

C. Evain,[1] F. Kaoudoune,[1] E. Roussel,[1] C. Szwaj,[1] M.-A. Tordeux,[2] F. Ribeiro,[2] M. Labat,[2] N. Hubert,[2] J.-B. Brubach,[2] P. Roy,[2] and S. Bielawski[1]

[1]*Univ. Lille, CNRS, UMR 8523—PhLAM—Physique des Lasers Atomes et Molécules, F-59000 Lille, France*

[2]*Synchrotron SOLEIL, Saint Aubin, BP 34, 91192 Gif-sur-Yvette, France*

(Received 3 February 2023; accepted 27 July 2023; published 5 September 2023)

Recent studies have demonstrated the effectiveness of feedback techniques in suppressing the bursting behavior caused by microbunching instabilities, leading to the stabilization of terahertz (THz) coherent synchrotron radiation (CSR) emission in storage rings. However, the use of feedback loops on the accelerator voltage without proper caution can lead to destabilization of the bunch position and result in beam losses, which limits the optimal feedback parameters. In this paper, we propose a solution to this limitation by introducing a second feedback loop on the phase of the accelerating voltage. The effectiveness of this strategy has been tested at the SOLEIL storage ring, representing a significant step forward in mitigating microbunching instability at high current charges.

DOI: 10.1103/PhysRevAccelBeams.26.090701

I. INTRODUCTION

The microbunching instability or coherent synchrotron radiation (CSR) instability is an ubiquitous phenomenon, that occurs in accelerator-based light sources, due to the interaction of the electrons with their own emitted radiation. When the peak current of the electron-bunch exceeds a threshold value, microstructures appear spontaneously in the bunch profile, leading to the emission of coherent synchrotron radiation at the microstructures wavelengths [1–6].

In storage rings, this coherent CSR emission usually occurs in the THz range, corresponding to microstructure wavelengths in the millimeter range. This phenomenon has been observed in a large number of facilities (for example see [7–10]), and studied with a special focus on its potential for users, given the high power of the source. CSR power is usually higher by several orders of magnitude than standard (incoherent) synchrotron radiation power [1,10–12].

However practical uses of such source have been largely hindered by the complex time-evolution of the emitted light. This is due to an instability coming from an interplay between an increase of the bunch length (due to the presence of the structures in the bunch) and the natural damping (due to the synchrotron radiation) [13]. As a direct consequence, the temporal evolution of the THz power presents a bursting behavior, which usually prevents the use of this source for synchrotron light source users.

A classical strategy used to prevent this bursting behavior is to configure the storage rings in the so-called low-alpha mode (with the parameter alpha being related to the longitudinal dispersion), where the bursting behavior is less pronounced [9,14]. However, a drawback of this solution is the necessity to use electron-bunches with low charge, decreasing drastically the power of the synchrotron radiation at other wavelengths than in the terahertz range.

Another solution to remove the bursting behavior—while maintaining the microstructures—consists in using a feedback control strategy. It has recently been demonstrated that using a feedback loop (composed of a measure of the THz power and acting on the amplitude of a radio-frequency accelerating cavity), the bursting behavior can be removed or largely decreased [15]. From a conceptual point of view, this process consists in stabilizing an already existing solution in the system, which is intrinsically (i.e., without feedback loop) unstable [16]. This solution is characterized by a regular formation of the microstructures (i.e., without bursting behavior), leading to a quasiconstant coherent THz emission. This process has also the advantages to be a noninvasive process: when the stabilization is achieved, a very small amount of modification of the energy (brought by the rf cavity) is necessary to maintain the stabilization.

In this context, studies at KARA storage ring, using adaptive feedback methods and modification of the rf field have also been carried out in order to modify the CSR THz emission properties [17–19].

In this article, we focus on one limitation that occurs using the feedback loop strategy, and show that it can be

overcome with an adaptation of the first version of the feedback setup. For some feedback parameters, we observe experimentally that the feedback loop causes an electron beam oscillation in the transverse horizontal direction, and this oscillation can be high enough to move the beam outside the storage ring acceptance. We show here that an additional feedback loop can stabilize the bunch position and suppress this phenomena. Hence, this dual control permits to access new area of feedback parameters, and appears to efficiently reduce the THz fluctuations. This method has been experimentally tested at the Synchrotron SOLEIL.

II. PROBLEM OF THE BEAM LOSS DUE TO THE FEEDBACK LOOP

During the microbunching instability, the microstructures generally appear with a bursting behavior (see for example Fig. 2(a), for $t < 0$), due to a variation of the bunch length, which is a consequence of the interplay between the presence of the microstructures and the natural synchrotron damping [13,20].

As described in Ref. [15], the feedback method used to suppress this bursting behavior is based on the principle of increasing the bunch length (and thus to decrease the bunch peak current) when the microstructures become too strong, and inversely of decreasing the bunch length when the microstructures are too weak. In the best cases, it permits to stabilize a solution of the system where the microstructures develop regularly (and thus where the bursting behavior does not appear). In most cases, this solution has unstable properties and cannot be observed without the feedback.

Technically, the THz power $P_{\mathrm{THz}}(t)$ is used as a measure of the strength of the microstructures in the bunch (cf. Fig. 1), and is used to calculate the feedback signal $\Delta V(t)$. In this study, we use a delayed feedback (or Pyragas method [21]), and $\Delta V(t)$ is calculated with the following formula:

$$\Delta V(t) = G_V[X(t) - X(t-\tau)], \tag{1}$$

$$\frac{dX}{dt} = \frac{1}{\tau_{LP}}[P_{\mathrm{THz}}(t) - X(t)], \tag{2}$$

with $X(t)$ the THz power filtered with a first order filter (see [15] for more details). G_V and τ are the gain and delay of the feedback, respectively, and τ_{LP} is the time constant of the filter (in this study $\tau_{LP} \sim 15$ μs). This feedback signal ΔV is used to modulate the amplitude of a rf cavity tuned in zero crossing mode (see right rectangle Fig. 1). The zero crossing mode permits to transform directly a modulation of the rf signal amplitude ΔV into a modulation of the rf signal slope that the electron bunch undergoes when it passes through the rf cavity, which acts then on the bunch length.

For the study at the Synchrotron SOLEIL, the THz power is recorded using a fast bolometer (with a 1 μs response time) at the THz/infrared beamlines AILES [22], and the calculation of the feedback signal is performed using a FPGA card (Red Pitaya STEMlab 125-14 board). The storage ring is setup in the configuration used generally for users operation, except that only a single bunch is circulating in the ring with a current I of about 9.7 mA (instead of 416 bunches and a total current of 500 mA). For this operation, the microbunching instability threshold I_{th} (measured experimentally) is about of 8.75 mA.

To observe the effect of the feedback, a scan of the two feedback parameters G_V and τ is performed automatically. The Fig. 2(i) shows the fluctuations of the THz power as a function of these feedback parameters (G_V and τ).

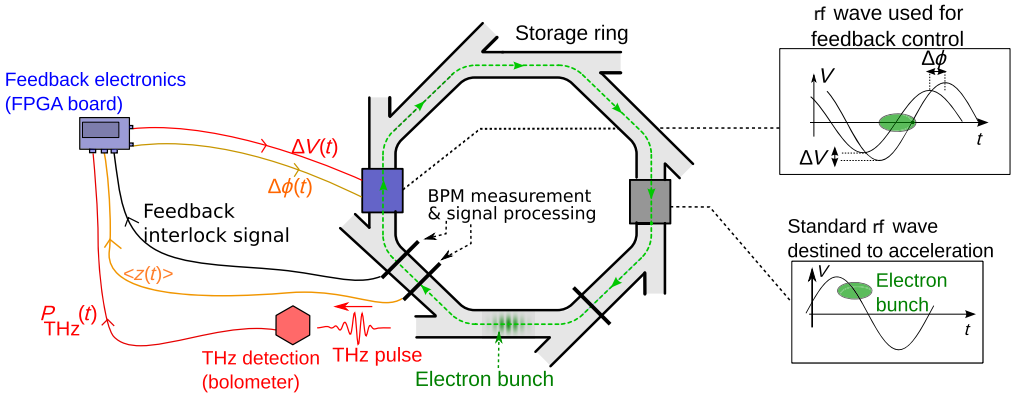

FIG. 1. Experimental setup of the feedback method (with dual feedback loops). An electron bunch, with a current higher than the instability threshold, is circulating in the storage ring. The first feedback loop, in red, (used to suppress the THz bursts) is composed of a measure of the THz power $P_{\mathrm{THz}}(t)$, the calculation of the feedback signal $\Delta V(t)$, and a change of the amplitude of a rf cavity tuned in a zero crossing mode (cf. upper right rectangle). The second feedback loop, in orange, (used to stabilize the bunch position) is composed of a measure of the longitudinal bunch position $\langle z(t)\rangle$, the calculation of the feedback signal $\Delta\Phi(t)$, and a change of the phase of the same rf cavity. The others rf cavities are tuned in a standard mode (cf. lower right rectangle). A feedback interlock signal, from beam position monitor (BPM) measurements is used to stop the feedback loops if the bunch transverse horizontal position exceeds a threshold value (details in methods of [15]).

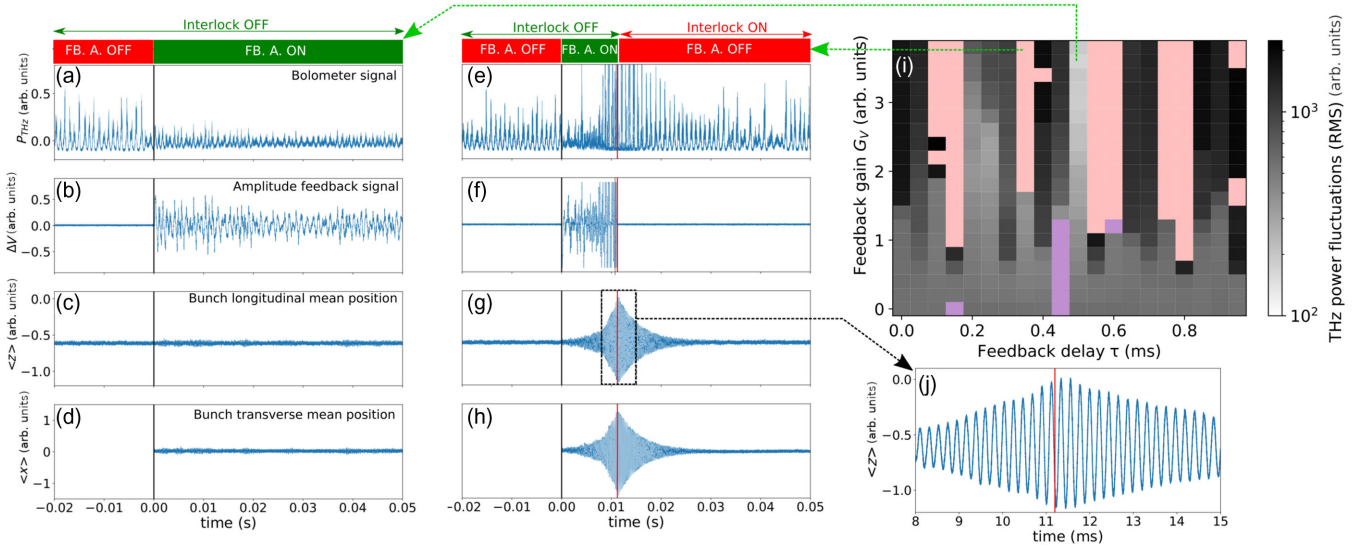

FIG. 2. (a–h) temporal evolution of several signals (THz power, bunch position, feedback signal) when the feedback loop is activated (at $t = 0$), in the two cases of successful and failing control. (a, e) THz power $P_{\mathrm{THz}}(t)$, (b, f) feedback signal $\Delta V(t)$, (c, g) longitudinal bunch position $\langle z(t)\rangle$, and (d,h) transverse horizontal bunch position $\langle x(t)\rangle$ (see Appendix A for recording details). (a–d): case of the maximal decrease of the THz power fluctuations thanks to the feedback loop ($G_V = 3.6$, $\tau \simeq 0.5$ ms). (e–h): case of an increase of the fluctuations due to the feedback ($G_V = 3.8$, $\tau \simeq 0.35$ ms), inducing a stop of the feedback loop (at $t \sim 0.012$ ms, indicated by the red vertical lines) thanks to a feedback interlock system (based on signal shown in h). (j): zoom of the figure (g). (i): rms fluctuations of the filtered THz power [given by Eq. (2)] (in color scale) in function of the feedback parameters G_V and τ; pink area corresponds to situations where the feedback has been stopped due to the feedback interlock system. Purple area correspond to unexpected interlocks (regarding the bunch position displacement), see Appendix B for details.

It appears that some feedback parameters allow to decrease significantly the THz fluctuations, as shown in the Fig. 2(a), with a reduction of some frequency components down by 10^3 (see Appendix C). In this situation, the bunch position doesn't move significantly. This can be observed on either the longitudinal bunch position $\langle z(t)\rangle$ shown in the Fig. 2(c), or on the transverse horizontal bunch position $\langle x(t)\rangle$ shown in the Fig. 2(d) (these two signals are obtained using a BPM, and are correlated which each other due to dispersion phenomena).

On the contrary to this successful control, there are also configurations—in particular for high gain feedback values—where the feedback destabilizes the system, i.e., it strongly increases the THz fluctuations and also increases the displacement of the bunch position. An example of such a situation is displayed on the Figs. 2(e)–2(h), where after the feedback is activated (at $t > 0$), the THz fluctuations increase strongly. The feedback also causes the bunch position to oscillate at the synchrotron frequency [see Fig. 2(j)]. The amplitude of this oscillation growths with time, and if the feedback is not stopped, the electron bunch ends being lost. In the Figs. 2(e)–2(h), the feedback is stopped at $t \sim 1.12$ ms thanks to a feedback interlock system, based on the BPM signal $\langle x(t)\rangle$ (displayed Fig. 2(h) and details in methods of [15]).

In this situation, we can observe that the feedback signal ΔV includes a frequency component at the synchrotron frequency (see Appendix D). We can deduce that the feedback loop excites the system at this frequency. Since the bunch centroid in the longitudinal phase-space can be modelized (without collective effects) by a damped harmonic oscillator with a resonant frequency at the synchrotron frequency [23], an excitation at this frequency can make this system unstable. The excitation of the bunch centroid could be realized by the rf cavity, where a shift—even extremely small compared to the perfect zero crossing mode—can make move the bunch centroid in the longitudinal position.

From a more general point of view, it is known that feedback delay can—for some parameters—destabilize some dynamical systems (see for example, [24]), as it is the case here.

In Fig. 2(i), the areas where the feedback interlock has been activated (i.e., where the feedback loop has been stopped) are displayed in red. Thus this phenomena of destabilization of the bunch position by the feedback may prevent the access to a large area of feedback parameters (in particular for high feedback gain values), and it appears in particular at higher bunch current (see supplementary information of [15] for a situation closer to the instability threshold).

In the next section, we describe a strategy to suppress this effect using a second feedback loop.

Notice also that in the THz signal, additionally to the variation at the burst frequencies, it exists a faster modulation of the THz signal due to the rotation of the

microstructures in the phase-space (see [25] for more details). For this experiment, this frequency is at about 80 kHz and is filtered during the process of calculation of the feedback signal (see Eq. (2)), and thus it does not play a role in the feedback process.

III. ADDITIONAL FEEDBACK TO STABILIZE THE BUNCH POSITION

The second feedback loop aims at suppressing the bunch displacement in the longitudinal direction. This second feedback loop is composed of a loop between a measurement of the longitudinal bunch position $\langle z(t)\rangle$ and the modification of the phase of a rf-signal $\Delta\phi$ (which acts on the longitudinal position $\langle z\rangle$ of the bunch).

In this article, this feedback loop is called the phase-feedback loop (versus the amplitude-feedback loop for the previous feedback loop). The same rf-cavity is used for the two feedback loops, the first acting on its amplitude and the second acting on its phase (see Fig. 1). A proportional feedback is used to calculate the feedback signal $\Delta\phi$:

$$\Delta\phi(t) = G_\phi[\langle z(t)\rangle - z_{\mathrm{ref}}] \tag{3}$$

with G_ϕ and z_{ref} the gain and the reference value of the feedback, respectively, and $\langle z(t)\rangle$ the longitudinal bunch position. Finally, this feedback signal $\Delta\phi$ is also calculated using the same FPGA card used for the amplitude-feedback loop.

A. Below instability threshold, to find phase-feedback parameters

In order to find the optimum phase-feedback loop parameters z_{ref} and G_ϕ, the bunch current is chosen below the microbunching instability current threshold (here $I \sim 7$ mA), and the amplitude-feedback loop is disabled ($G_V = 0$). Then, the method to find the parameters consists of two steps.

First, the phase of the signal in the rf cavity is modified, in order to add a constant value K (i.e., $\Delta\phi = K$). It induces a movement of the bunch in the longitudinal direction, and we wait for the bunch position to reach its new equilibrium position (this step is not shown in the figures).

Second, the rf phase is suddenly pushed back to its initial value, and at the same time the phase-feedback loop is activated [with $\Delta\phi(t)$ calculated using Eq. (3)].

In the case where the phase-feedback loop is not applied (i.e., $G_\phi = 0$ for $t > 0$, see Fig. 3(b)), the bunch comes back to its equilibrium position with an oscillation at the synchrotron frequency and with an exponential decay due to the synchrotron radiation damping (see Fig. 3(a)).

If the phase feedback loop is applied with optimal parameters, the bunch goes to its final position much faster and without oscillation [see Fig. 3(c)], as in an aperiodic regime. In this case, the feedback signal $\Delta\phi$ is not null but small (see Fig. 3(d) for $t > 0$).

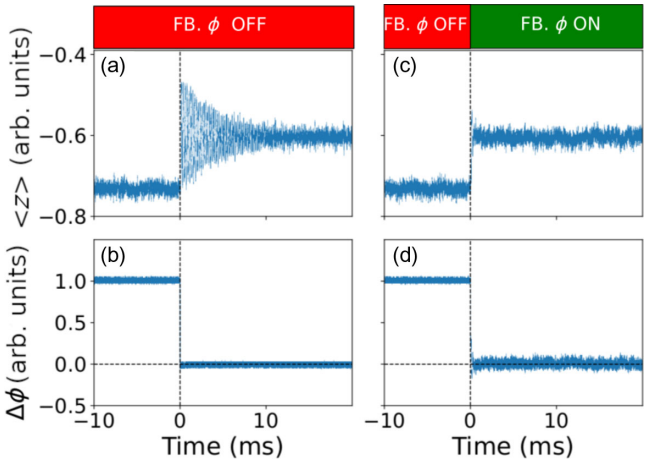

FIG. 3. (a, c) Electron bunch longitudinal position $\langle z(t)\rangle$ when the phase of the rf-signal is suddenly shifted at $t = 0$. In (a) the feedback on the phase is not activated. In (c), the feedback on the phase is activated just after the shift of the rf-phase signal (at $t = 0$). (b) and (d): associated phase-feedback signal $\Delta\phi(t)$. Note that in this part, the amplitude-feedback loop is disabled ($G_V = 0$).

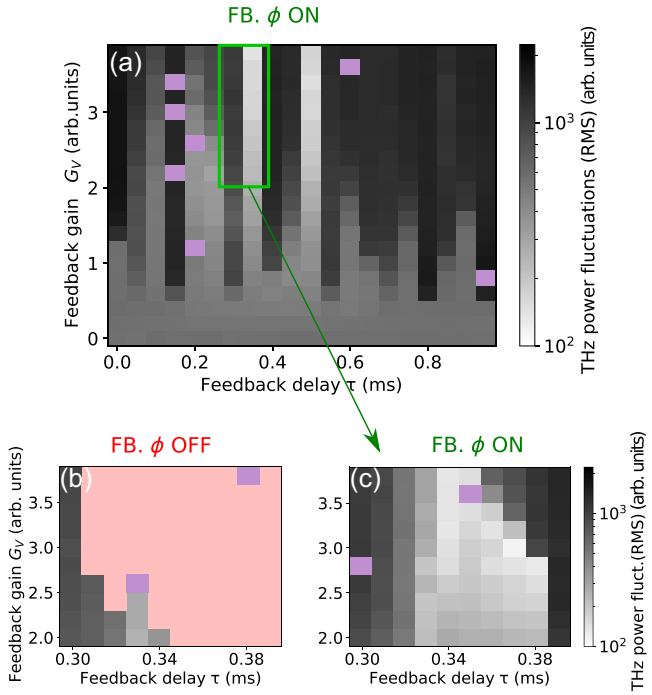

FIG. 4. (a) fluctuations of the THz power (colorscale) as a function of the amplitude-feedback loop parameters τ and G_V, in the same conditions than in Fig. 2(i) except that the phase-feedback loop is activated. Pink area are still associated to a situation where the feedback interlock system has been activated. (c) zoom (with a higher resolution) on a parameter area (located between the green rectangle in [Fig. 4(a)]). (b) same than in [Fig. 4(c)] but with the phase-feedback loop disabled ($G_\phi = 0$).

B. Above the instability threshold: Effect of the phase-feedback loop

As a last step, this phase-feedback loop is used when the bunch current is above the instability threshold (more precisely using the same current than in the Sec. II, $I \simeq 9.7$ mA). This phase-feedback loop is used together with the amplitude feedback loop. As on the Sec. II, the amplitude-feedback parameters G_V and τ are scanned systematically. The phase-feedback parameters G_ϕ and z_{ref} are fixed, with the values found previously.

The Fig. 4 shows the result of this scan, where we can see that the phase feedback permits to prevent the activation of the feedback interlock system.

Some new accessible feedback parameters appears to have a good efficiency to decrease the THz fluctuations. In fact, the best configuration to decrease the THz fluctuations is in an area which is not possible to probe without the phase-feedback (see Figs. 4(b) and 4(c) for a detailed view of this area with and without the phase-feedback loop).

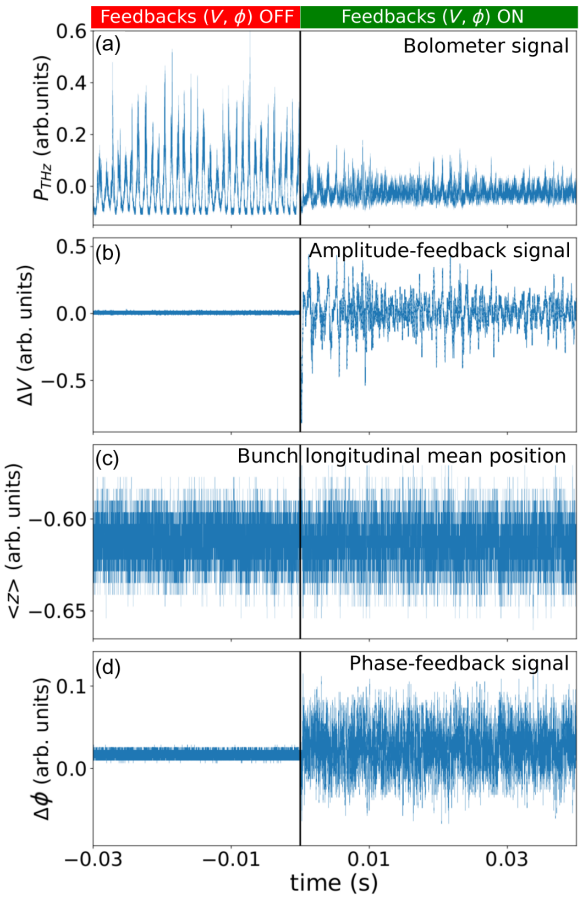

FIG. 5. Temporal signals for the case of the maximal decrease of the THz power fluctuations thanks to the two feedback loops ($G_V = 3.8$, $\tau \simeq 0.35$ ms). (a) THz power $P_{\mathrm{THz}}(t)$, (b) feedback signal $\Delta V(t)$, (c) longitudinal bunch position $\langle z(t) \rangle$, and (d) feedback signal $\Delta\phi(t)$.

The different temporal signals associated to this case of minimal THz fluctuations are displayed on the Fig. 5. It permits to reduce the THz power rms fluctuations by about 20%, compared to the best case without the phase-feedback loop [signals displayed in the Figs. 2(a)–2(d)].

As a comparison, the signals for the same configuration but without the phase-feedback loop are displayed Figs. 2(e)–2(h).

Thus, the phase-feedback loop permits to prevent the destabilization at the synchrotron frequency (by forcing the system to stay at the same position), and then it allows the amplitude feedback loop be able to remove the bursting behavior. From a nonlinear dynamical point of view, the different regimes can be explained as follow: without feedback loop, there are unstable modes in the system (i.e., eigenvectors associated to unstable eigenvalues), inducing the bursting behavior. For some parameters, the amplitude feedback loop permits to stabilize these previously unstable modes [case of Fig. 2(a)]. For other parameters [case of Fig. 2(b)], it appears that the amplitude feedback loop has another effect: it also destabilizes some previously stable modes (associated to an oscillation of the bunch longitudinal position at the synchrotron frequency), making finally the system unstable. The phase-feedback loop permits to stabilize this mode—making the system stable (without oscillation at the synchrotron frequency and without bursting behavior).

Finally, this second feedback loop permits also to improve slightly the efficiency of the control process (decrease of about 10% ot the THz power fluctuations) for feedback parameters allowing an efficient control without the phase-feedback loop.

IV. CONCLUSION

The bursting behavior generally observed during the microbunching instability in storage rings can be removed or can be significantly decreased using a feedback loop, composed of a measurement of the THz power and a modification of the amplitude of the signal in a rf cavity. However, this same feedback loop can—for some parameters—make the bunch oscillate strongly, and for such cases, no diminution of the THz fluctuations can be achieved. It appears that such a situation appears more often when the bunch current is increased (see for example Fig. 2 of the supplemental material of [15]), thus reducing importantly the feedback parameters that can be used.

To remove to a large extent this phenomena, we have shown that a second feedback loop can be added, allowing to stabilize the bunch position in the longitudinal direction. This feedback loop is based on a measurement of the bunch position and a modification of the phase of the rf signal used for the first feedback loop. It permits to access a larger ensemble of feedback parameters, with some of them interesting in term of diminution of the THz power fluctuations. This method is a step forward to effectively

stabilize electron bunches at high current, as it allows to strongly diminish the THz power fluctuations caused by the microbunching instability.

ACKNOWLEDGMENTS

The PhLAM team was supported by the following funds: Ministry of Higher Education and Research, Nord-Pas de Calais Regional Council, and European Regional Development Fund (ERDF) through the Contrat de Plan État-Région (CPER photonics for society), LABEX CEMPI project (ANR-11-LABX-0007), and the ANR-DFG ULTRASYNC project (ANR-19-CE30-0031).

APPENDIX A: DETAILS ON THE RECORDING OF THE TEMPORAL SIGNALS

Temporal signals are recorded systematically during a scan of the feedback parameters. For each feedback parameters (G_v, τ), four signals are recorded thanks to an oscilloscope placed in the AILES beamline (using a 104MXI TELEDYNE-LECROY oscilloscope): the THz power $P_{\mathrm{THz}}(t)$ (negative value of the bolometer signal is due to the detection principle of this detector which is an AC detector), the mean bunch position $\langle z \rangle$ (the offset of this measure is due to the fact that the bunch position is not associated to the zero value of the system of measurement), the feedback signal ΔV and the feedback signal $\Delta\Phi$.

The sampling rate is of 5 MS/s, and to remove frequency components higher that this sampling rate, an analog first order filter (with $f_c \sim 1$ MHz) is used (for each channel of the oscilloscope).

In parallel to the recordings with the oscilloscope, the turn-by-turn bunch transverse position $\langle x \rangle$ is recorded in the control room by the beam position monitor (BPM) system. This acquisition is triggered when the amplitude feedback is activated (i.e. for $t > 0$ in the Fig. 2).

APPENDIX B: FEEDBACK INTERLOCK SYSTEM AND MAP OF THE MAXIMUM VALUE OF THE BPM SIGNAL

The same position data $\langle x \rangle$ is filtered and down-sampled by the BPM processor, and then is compared to a position threshold. When the bunch transverse position exceeds this threshold value, an interlock signal is generated. In the experiment, this feedback interlock signal is used to stop the feedback(s). However, in some few cases, the feedback interlock has been activated unexpectedly. This can be observed with the color maps of the Fig. 6, representing the maximum value of the BPM signal for each feedback parameters (associated to the color maps of the Figs. 2 and 4). It appears that for some few cases, indicated in purple, the feedback interlock has been activated whereas the maximum value of the BPM signal has a value well below values associated to an expected interlock (typical turn-by-turn maximum BPM value for an expected interlock is about 1.5 mm). To detect unexpected feedback interlock, we use a maximum value below 0.5 mm: if the

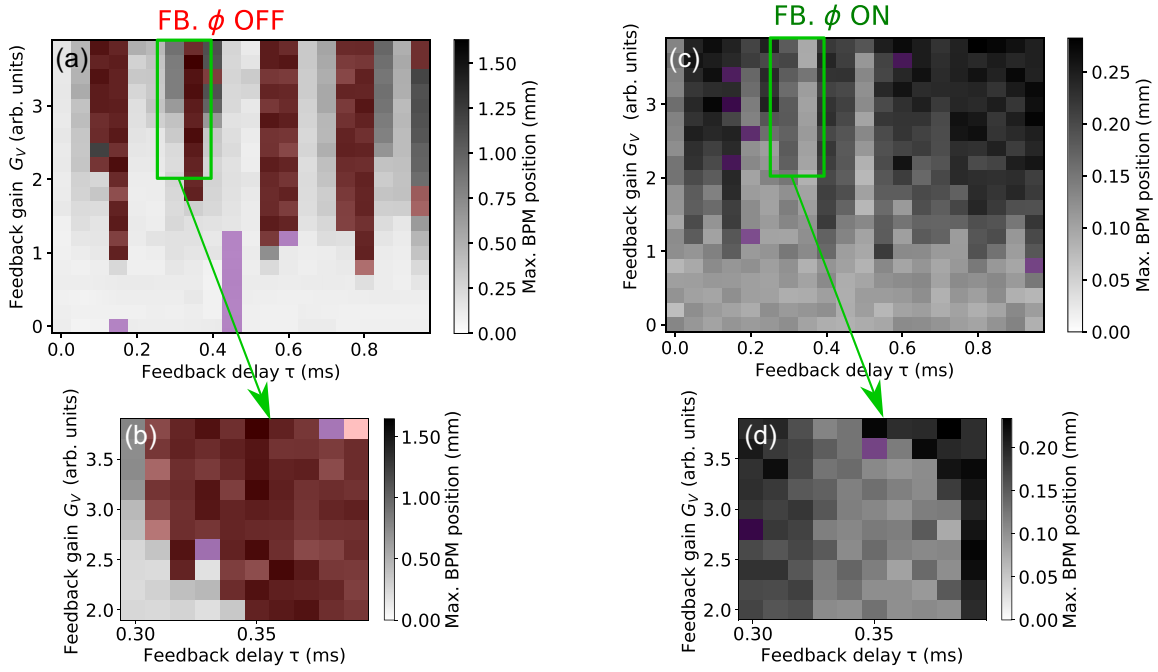

FIG. 6. Color scale: maximum value of the BPM signal versus the feedback parameters G_V and τ. Red area are associated to a "real" feedback interlock (with an high maximum value of the BPM signal) and the purple area are associated to "false" feedback interlock (with a low maximum value of the BPM signal). The map (a) is linked to the map of the Fig. 2 of the article; the maps (b), (c), (d) are linked to the map of the Fig. 4 of the article.

feedback interlock has been activated and the maximum value of the BPM signal is lower than this threshold value, the feedback interlock is considered as unexpected). This analysis permit to dismiss parameters in this situation and permit to clarify the analysis of the maps presented Figs. 2 and 4.

APPENDIX C: FREQUENCY COMPONENTS OF THE BOLOMETER SIGNALS

The Fig. 7 shows the norm of the Fourier transform of the bolometer signal, in several cases. Blue lines are associated to a case without feedback loop. Red lines

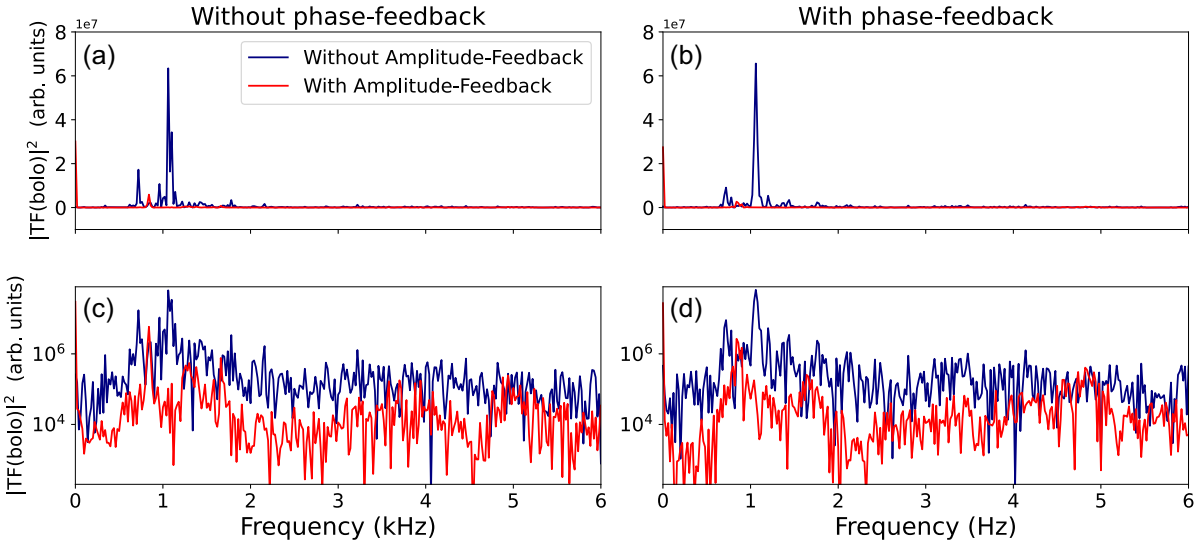

FIG. 7. Norm of the Fourier transform of the bolometer signals. In blue lines, situations without feedback. In red lines, best reduction of the THz fluctuations, in the case (a, c) without the phase-feedback (associated to the temporal signal shown Fig. 2(a)), and in the case (b, d) with the phase-feedback (associated to the temporal signal shown Fig. 5(a)). Top: linear vertical scale. Bottom: logarithmic vertical scale.

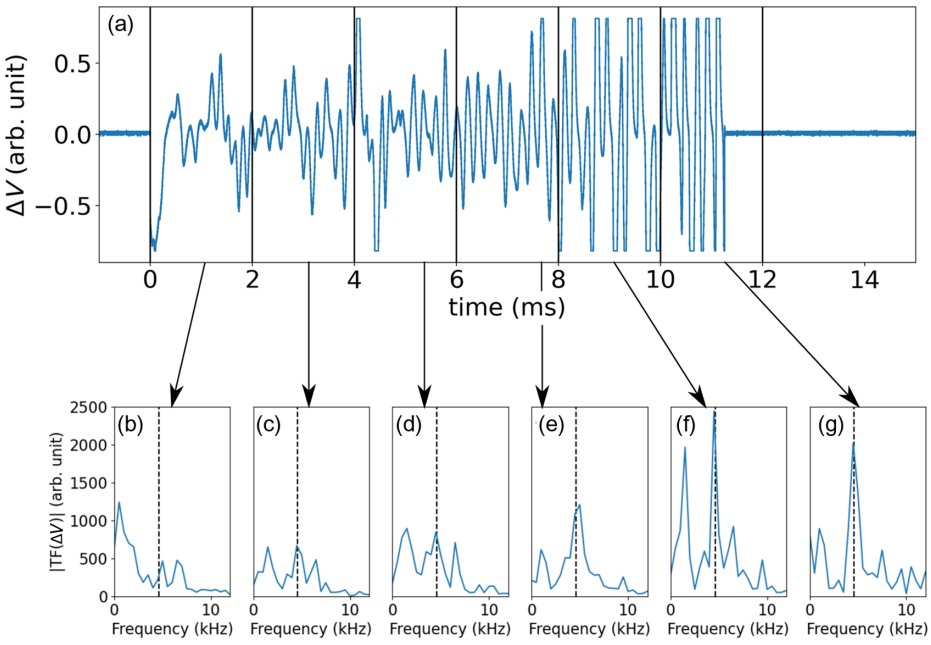

FIG. 8. (a) Temporal evolution of the amplitude feedback $\Delta V(t)$, for a situation of a destabilization by the amplitude-feedback loop (corresponding to a zoom of the Fig. 2(f)). (b–g) Absolute value of the Fourier transform of the amplitude-feedback signal, for the six time windows indicated by the arrows. In these figures, we can see the apparition of a frequency component at the synchrotron frequency (at about 4.6 kHz, indicated by the vertical lines in each figure).

are associated to the best reduction of the THz fluctuations; on the left column, when only the amplitude feedback is applied [a part of the associated temporal signal is shown Fig. 2(a)]; and on the right column, with the phase-feedback applied (a part of the associated temporal signal is shown Fig. 5(a)).

APPENDIX D: FREQUENCY COMPONENTS OF THE FEEDBACK SIGNAL FOR A SITUATION WITH A DESTABILIZATION

The Fig. 8 shows the temporal evolution of the feedback signal [Fig. 8(a)] in a case of destabilization by the feedback [zoom of the Fig. 2(f)]. The Fourier transform of this signal for several time windows [Figs. 8(b)–8(g)] permits to see the apparition and the presence of a frequency component at the synchrotron frequency (at about 4.5 kHz).

[1] J. M. Byrd, W. P. Leemans, A. Loftsdottir, B. Marcelis, M. C. Martin, W. R. McKinney, F. Sannibale, T. Scarvie, and C. Steier, Phys. Rev. Lett. **89**, 224801 (2002).

[2] A. W. Chao and M. Tigner, *Accelerator Physics and Engineering* (World Scientific, Singapore, 1999).

[3] G. Stupakov and S. Heifets, Phys. Rev. ST Accel. Beams **5**, 054402 (2002).

[4] S. Di Mitri and S. Spampinati, Phys. Rev. Accel. Beams **20**, 120701 (2017).

[5] Z. Huang and G. Stupakov, Nucl. Instrum. Methods Phys. Res., Sect. A **907**, 182 (2018), advances in Instrumentation and Experimental Methods (Special Issue in Honour of Kai Siegbahn).

[6] E. Roussel, E. Ferrari, E. Allaria, G. Penco, S. Di Mitri, M. Veronese, M. Danailov, D. Gauthier, and L. Giannessi, Phys. Rev. Lett. **115**, 214801 (2015).

[7] W. Cheng, B. Bacha, and G. L. Carr, Observation of microbunching instabilities using THz detector at NSLS-II, in *Paper presented at the 2019 International Beam Instrumentation Conference, Malmö, Sweden* (JACoW, Geneva, 2019), paper WEPP038, https://dx.doi.org/10.18429/JACoW-IBIC2019-WEPP038.

[8] M. Brosi, J. L. Steinmann, E. Blomley, T. Boltz, E. Bründermann, J. Gethmann, B. Kehrer, Y.-L. Mathis, A. Papash, M. Schedler *et al.*, Phys. Rev. Accel. Beams **22**, 020701 (2019).

[9] C. Evain, E. Roussel, M. Le Parquier, C. Szwaj, M.-A. Tordeux, J.-B. Brubach, L. Manceron, P. Roy, and S. Bielawski, Phys. Rev. Lett. **118**, 054801 (2017).

[10] J. Feikes, M. von Hartrott, M. Ries, P. Schmid, G. Wüstefeld, A. Hoehl, R. Klein, R. Müller, and G. Ulm, Phys. Rev. ST Accel. Beams **14**, 030705 (2011).

[11] J. Barros, C. Evain, L. Manceron, J.-B. Brubach, M.-A. Tordeux, P. Brunelle, L. Nadolski, A. Loulergue, M.-E. Couprie, S. Bielawski *et al.*, Rev. Sci. Instrum. **84**, 033102 (2013).

[12] M. Brosi, J. L. Steinmann, E. Blomley, E. Bründermann, M. Caselle, N. Hiller, B. Kehrer, Y.-L. Mathis, M. J. Nasse, L. Rota *et al.*, Phys. Rev. Accel. Beams **19**, 110701 (2016).

[13] A. Mochihashi, M. Hosaka, M. Katoh, M. Shimada, and S. Kimura, Observation of THz Synchrotron radiation bursts in UVSOR-II storage ring, Paper presented at the *2006 European Particle Accelerator Conference, Edinburgh, Scotland. Place of publication: Joint Accelerator Conferences Website* (JACoW, Genava, 2006), paper THPLS042.

[14] M. Abo-Bakr, J. Feikes, K. Holldack, G. Wüstefeld, and H.-W. Hübers, Phys. Rev. Lett. **88**, 254801 (2002).

[15] C. Evain and C. Szwaj, Nat. Phys. **15**, 635 (2019).

[16] E. Ott, C. Grebogi, and J. A. Yorke, Phys. Rev. Lett. **64**, 1196 (1990).

[17] T. Boltz, M. Brosi, E. Bründermann, B. Haerer, P. Kaiser, C. Pohl, P. Schreiber, M. Yan, T. Asfour, and A. S. Müller, Feedback design for control of the micro-bunching instability based on reinforcement learning, in *ICFA mini-Workshop on Mitigation of Coherent Beam Instabilities in Particle Accelerators (MCBI 2019)* (CERN, 2020), pp.227–229, http://cds.cern.ch/record/2752631.

[18] W. Wang, M. Caselle, T. Boltz, E. Blomley, M. Brosi, T. Dritschler, A. Ebersoldt, A. Kopmann, A. Santamaria Garcia, P. Schreiber *et al.*, IEEE Trans. Nucl. Sci. **68**, 1794 (2021).

[19] T. Boltz, Ph.D. thesis, Karlsruher Institut für Technologie (KIT), 2021, 54.11.11; LK 01.

[20] M. Venturini and R. Warnock, Phys. Rev. Lett. **89**, 224802 (2002).

[21] K. Pyragas, Phys. Lett. A **170**, 421 (1992).

[22] P. Roy, M. Rouzières, Z. Qi, and O. Chubar, Infrared Phys. Technol. **49**, 139 (2006).

[23] A. W. Chao, K. H. Mess, M. Tigner, and F. Zimmermann, in *Handbook of Accelerator Physics and Engineering* (World Scientific, Singapore, 2013).

[24] T. Balogh, I. Boussaada, T. Insperger, and S.-I. Niculescu, International Journal of Robust and Nonlinear Control (2021), https://hal.science/hal-03277678.

[25] E. Roussel, C. Evain, C. Szwaj, and S. Bielawski, Phys. Rev. ST Accel. Beams **17**, 010701 (2014).